Ultrasonic Imaging of Micro-Leaks and Seal Contamination in Flexible Food Packages by the Pulse-Echo Technique

AYHAN OZGULER, SCOTT A. MORRIS, and WILLIAM D. O'BRIEN, JR.

ABSTRACT

Reliable inspection of flexible food packages for micro-leaks and product contamination in the seal area is needed to prevent spoilage and safety hazard. Nondestructive testing by the ultrasonic imaging method, Backscattered Amplitude Integral (BAI), was evaluated for use in defect detection. Channel defects (6-15 μm in diameter) and simulated food strands (20-60 μm dia) perpendicular to the sealing direction were fabricated within the seal region of both all-plastic and foil-containing retortable pouches. Results showed that 17.3-MHz pulse-echo BAI-imaging detected channel defects (9.5-15 μm) and all strand-inclusion defects in both types of package materials.

Key Words: microleaks, package defects, retortable pouches, nondestructive evaluation, ultrasound imaging

INTRODUCTION

AN IMPORTANT REQUIREMENT FOR FLEXIble food packages is the complete fusion of opposing seal surfaces to prevent the entrance of microorganisms and moisture. Presence of water vapor, air bubbles, product, wrinkles, blisters and delamination in the seal region might cause a defective seal (Yamaguchi, 1990). Lampi et al. (1976) observed that occluded particles in the seal area resulted in the decrease in bursting strength of retortable pouch seals after 6 mo storage. Harper et al. (1995) showed that the minimum leak size that microorganisms could penetrate varied between 0.2 and 80 μm in diameter. This broad range was due to the different experimental procedures used to measure the critical defect size. Other results indicated that critical-leak dimensions were 10 μm in diameter and 10 mm in length (Blakistone et al., 1996). Harper (1995) found virtually the same results in a study that implied it was not a definitive procedure to determine minimum penetration size. Regulatory agencies require a near zero tolerance for pathogens in foods (Blakistone et al., 1996), and therefore a thoroughly reliable seal defect sensing system is required.

Destructive methods have been used to inspect the seal integrity of packages (Axelson et al., 1990; Chen et al., 1991; Floros and Gnanasekharan, 1992; Gnanasekharan and Floros, 1994). Warrick (1990) showed that more than 2% of total production volume in packaging operations and about 7% of the total operating time are lost due to destructive testing. Thus, destructive inspection is costly and only provides a statistical assurance of integrity. A reliable and low cost nondestructive technique is needed to evaluate the seal integrity of packages.

Ultrasonic techniques are common in the field of nondestructive evaluation. Low-power ultrasonic applications do not result in permanent change in the medium under evaluation; and may be used to measure defects (in steel and other metals), obstacles, anatomical structure, material properties and flow (Szilard, 1987). Ultrasonic transducers, devices which convert electrical energy to mechanical energy are used to make the measurements.

Two general ultrasonic techniques used for flaw detection are transmission and pulse-echo (reflection) techniques. In transmission, separate transmitting and receiving transducers are positioned on opposing sides of the specimen. The ultrasonic beam is propagated through the sample. When the beam is impeded by inhomogeneities within the sample, the amplitude decreases due reflection and scattering. Jarman et al. (1994) applied this technique to detect contaminants such as Teflon®, silicon grease, and meat fiber within the seal region of a flexible packaging material. In that study, an average reference signal was recorded from the undisturbed region of the seal, and the peak of signals from the seal was evaluated relative to the reference signal. A decrease in magnitude of the peak showed that the bond was not complete. However, they did not demonstrate either the minimum detectable limit or the detection of any microscale channel defects, which are important factors for in-line inspection of seals. Safvi et al. (1997) showed that the Scanning Laser Acoustic Microscope (SLAM), a transmission technique, detected 10 μm channel defects within the seal region of both polyethylene films and retortable plastic pouches at an ultrasonic frequency of 100 MHz.

In the ultrasonic pulse-echo technique, an ultrasonic pulse is propagated into the sample, and the reflected pulse (echo) produced by inhomogeneities and flaws is received back by the same transducer (Szilard, 1987). This method is used to detect cracks, folds, inclusions, laminations, partial welds, voids, segregations, shrinks, porosity, and flaking in metals. Jarman et al. (1994) indicated that the pulse-echo technique probably would not be sufficiently sensitive to detect very fine flaws (such as ~1.0 mm^2 meat fiber) in the seal area of thin flexible packaging materials (total seam thickness was 185 μm). However, studies have shown 17.3 MHz pulse-echo Backscattered Amplitude Integral (BAI)-mode imaging technique (Raum et al., 1998); Ozguler et al., 1998); Frazier et al., 1998) could reliably detect channel defects (as small as 10 μm) within the seal region of retortable plastic pouches (total thickness 220 μm). In this technique, the BAI value for each scan point was calculated by integrating the envelope of the received echo signal. The BAI value was then proportional to the square root of the backscattered energy. As long as the seal region of the package was flawless and its surfaces smooth and parallel, the BAI value would be virtually constant. However, any discontinuities could cause the value to vary, and the variation was visualized by a gray mode BAI-image. Although successful in detecting defects as small as 10 μm in diameter, its absolute lower detection limit and detection ability for different packaging materials have not be reported.

Our objective was to evaluate the BAI-mode imaging technique with two flexible packaging materials (transparent all-plastic and opaque foil-containing retort pouches); with two types of defects of different sizes; and to determine its detection limits. The two defect types used were channel defects (6-15 μm), and inclusion defects, i.e., tendons (20-60 μm) excised from the tails of laboratory mice as the simulated material for food particles such as meat fiber that might be caught in the seal region of a package.

Author Ozguler is with the Dept. of Food Science & Human Nutrition, author Morris is with the Dept. of Food Science & Human Nutrition and Agricultural Engineering, and author O'Brien is with the Dept. of Electrical & Computer Engineering, Biosocoustic Research Laboratory, Univ. of Illinois, Urbana, IL, 61801. Direct inquiries to Dr. Scott A. Morris, Dept. of Food Science & Human Nutrition, Univ. of Illinois, 1304 W. Pennsylvania #382-G, Urbana, IL 61801.

MATERIALS & METHODS

Sample preparation

Two retortable pouch materials, an all-plastic and a foil-containing composite film were studied. The material composition of the all-plastic sample was nylon/polyvinylidene chloride/polypropylene (Fuji Tokushu Shigyo Co. Ltd., Seto Aichi, Japan) with a film thickness of 110 µm. It was optically transparent. The other material was opaque, and its composition was Polyester/Aluminum foil/Polypropylene (American National Can Company, Chicago, IL) with a film thickness of 120 µm. Polypropylene was the heat-sealing layer of both pouches. PVDC and aluminum foil, middle layers of each material, provide a barrier to chemical substances. Polyester and nylon, the outer layers, give strength, resistance to shear, chemical resistance, barrier to gases, oils and fats, and scuff resistance to the printed surface (Paine and Paine, 1983).

To fabricate different sized channel defects (air-filled and water-filled), tungsten wires (6, 10 and 15 µm in diameter: California Fine Wire Company, Grover City, CA) were used. These wires were positioned transverse to the sealing direction, sandwiched between two layers of pouch materials, and then sealed using an automatic band sealer (Doboy HS-C42051, Doboy Co., New Richmond, WI). In band sealing (Fig. 1), endless stainless steel bands (with nonstick teflon coating) guided and pressed the two layers of package material between the heated sealing bars. The heat passed through the bands and into the pouch material, softening it to seal. The pouch material then traveled between a pair of air-cooled bars, where the sealed area was cooled rapidly. The speed of the machine was 5.0 m/min, and the temperature for sealing was 132°C for all-plastic and 152°C for foil-containing pouches. The seals were cooled in air for (5 min before removing the wire. In order to create the air-filled channel defects, the tungsten wire was removed with the specimen in air. For water-filled channel defect creation, the samples were immersed in water, and the wire was then removed, drawing water into the channel. After wire removal, the channel ends were sealed with the band sealer to keep the water inside the channel defect.

Defects that include food material were simulated by the use of small animal tendons (Beckman Institute's Animal Care Facility, Urbana, IL) since the extraction of small tendon strands was much easier than that of meat fibers. Each tendon was placed transverse to the sealing direction, sandwiched between two identical packaging films, and heat-sealed. Both ends of the defect region were sealed to protect from any interaction of inclusion material with water during the experiment. Six water-filled and six air-filled channel defect samples (~6-15 µm), and three tendon defects (~20-60 µm) were fabricated for each packaging material, to give a total of 30 samples.

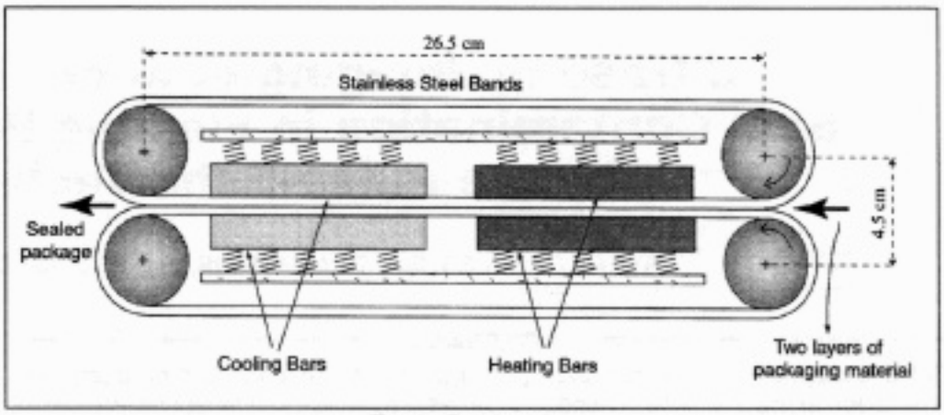

Fig. 1—Band sealer.

Sample validation

The size of the channels and tendons within the seal area of both packages was determined by light transmission microscope images with a calibration grid (Reicher Jung: 2 mm divisions into subdivision of 10 µm). A Nikon Optiphot-2 light microscope, Sony CCD color video camera, RasterOps frame-grabber board, Macintosh IIci computer, and Adobe Photoshop software were used to capture images into a high quality digital format.

Defect sizes were measured from both top and side views. Those from the side view were measured after samples were cut transverse to the longitudinal axis of the defect with a cyrostat (Lipshaw Manufacturing Company, Model no. 1500, Detroit, MI). Samples were frozen to -70°C (Forma Scientific, Model no. 80478-006, OH) for about 30 min before cutting to minimize distortion.

Ultrasound data acquisition

A 5-axis (3 linear and 2 rotational axes) precision positioning system with a linear positional accuracy of 2 µm and a rotational positional accuracy of 0.01° (Daedal Inc., Harrison City, PA) was controlled (Fig. 2) by a host PC (ZEOS 66 MHz 486). The sample was submersed in a degassed water tank (20°C), and its surface was positioned normal to the direction of the propagated sound beam. A pulser-receiver (Model 5800, Panametrics, Waltham, MA) operating in pulse/echo mode controlled by the PC was used to produce the 300 V monocycle pulse which excited a spherically focused, 6.35-mm ultrasonic transducer (Panametrics V317, Waltham, MA). The measured center frequency of the transducer was 17.3 MHz, the focal length was 12.7 mm, the -6 dB transmit-receive beam width of the focus was 176 µm, the -6 dB depth of focus was 2.42 mm, and the -3 dB fractional bandwidth was 27.4% (Raum and O'Brien, 1997). The received echo signal was amplified (20 dB), bandpass filtered (1-35 MHz) by the pulser-receiver, and then displayed (500Ms/s) on a digitizing oscilloscope (LeCroy 9374L, Chestnut Ridge, NY). The PC via IEEE-488 retrieved the digitized echo waveforms from the oscilloscope, and the stored waveforms were transferred to a SUN Sparc 20 workstation for off-line processing.

The time-of-transition (TOT) for the sound beam in the water was calculated by

$$TOT = [2 \times z(t)]/c_w \qquad (1)$$

where z(t) is the axial distance, and c_w is the speed of sound in the water (1483 m/s at 20°C, Kinsler et al., 1982). When the sample was properly positioned, the TOT was 17.16 µs at the focal length of z(t)=12.7 mm. The datum for each scan point was acquired and stored between TOT=16.8 and 17.8 µs to include the sample thickness.

The image data were collected in a rectangular grid pattern by moving the transducer relative to the fixed-position sample (Fig. 3). The horizontal grid spacings on the rectangular surface of the sample were 30 µm and vertical spacings 100 µm. The horizontal direction on the rectangle was parallel to the sealing direction, and the vertical direction was parallel to the longitudinal axis of the defect. The rectangular size of each sample was different, and its range varied from 1.0 mm (vertical direction) × 2.0 mm (horizontal direction) to 1.5 mm × 3.0 mm. If the size was, for example, 1.0 mm × 1.5 mm, the number of waveforms (Radio frequency (RF) echo signals) was 50 (1.5 mm/30 µm) in the horizontal direction and 10 (1.0 mm/100 µm) in the vertical direction for a total of 500. Since each waveform included 512 data points, the three dimensional data set for this specific example would contain 500 × 512-point RF data acquisitions.

BAI-mode image production

Hilbert transformation of the reflected RF signal (Fig. 4a) produced the envelope of the

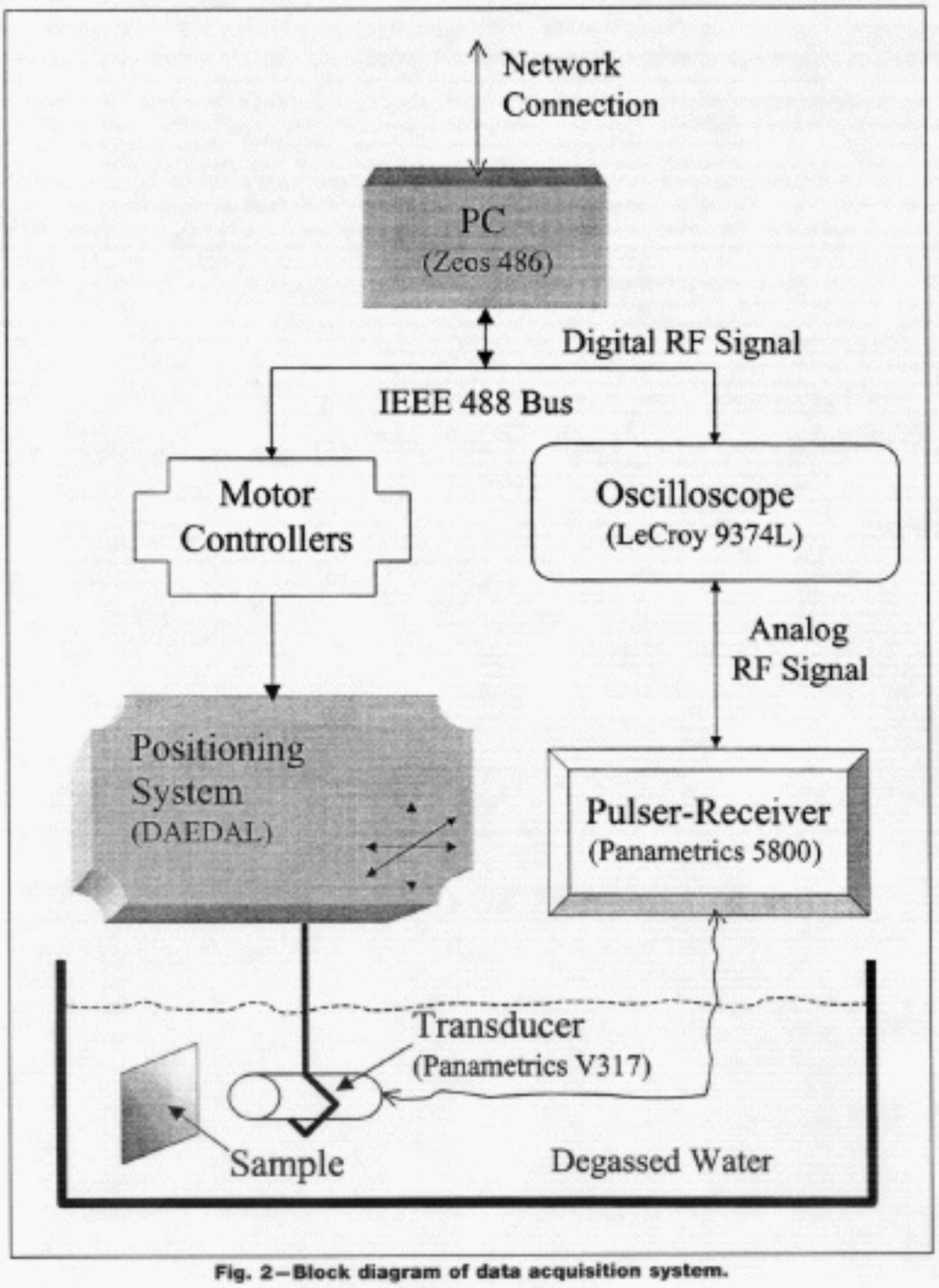

Fig. 2—Block diagram of data acquisition system.

signal, and the BAI value was calculated by integrating the envelope between 16.8 and 17.8 μs, which corresponds to the area under the curve (Fig. 4b). This calculation reduced the 3-D data set to a 2-dimensional BAI-value matrix. The matrix was normalized by dividing each BAI value by the maximum BAI value obtained in that matrix to provide the gray scale image. It was observed that the pixel size (100 μm × 30 μm) of the image was so large that the image was not smooth, and each pixel in the image was sharp, which made the detection of the defect difficult. Therefore, this matrix was interpolated to decrease the pixel size and make it approximately square. The interpolation was by a factor of 2 in the direction horizontal to the image rectangle (30 μm/2) and by a factor of 7 in the direction vertical to the image rectangle (100 μm/7). After interpolation, the corresponding pixel sizes became 14.3μm × 15.0 μm with the number of rows and columns in the BAI-value matrix of 70 (10 by 7) and 100 (50 by 2), respectively. The final image matrix was then normalized to yield the gray scale image. Image processing was performed using MATLAB((The Math Works, Inc., Natick, Mass.).

Statistical analysis

The maximum BAI value (BAImax), which was used to normalize the BAI-value matrix before producing the gray scale image, was determined from all-plastic, and from foil-containing retortable pouches. The average of BAImax values was calculated for each packaging material. The ability of the BAI technique to distinguish two packaging materials was evaluated by comparing their average BAImax value using the Analysis of Variance (ANOVA at a significance level of α=0.05) test. All statistical calculations were performed using Microsoft Excel© 97.

RESULTS

Lateral size of defects

Although the top view image of defects in the transparent all-plastic retort pouch was captured by the light microscope, that in the foil-containing pouch could not be detected due to the material opacity. The light transmission microscope image of an air-filled channel defect within the seal area of the all-plastic pouch (Fig. 5a) shows a lateral defect of 14.5 μm whereas the diameter of the tungsten wire used to create this defect was 15.0 μm. Lateral size of channel defects in the all-plastic seal area was, at most, 5% smaller than the wire diameter. Tendon defect lateral size in the transparent all-plastic pouches varied along the tendon due to its natural structure, and thus the smallest lateral size was recorded. Figure 5(b) shows a tendon defect (smallest lateral size ~20 μm) within the seal region of the all-plastic pouch. The dashed line shows the location where the size was measured.

Size measurements from the side view

Eight of 24 channel defect samples (both all-plastic and foil-containing) could not be detected from the side view by light transmission microscope, so the size from the cross section could not be validated. This was due to the shear deformation of the packaging material on the cut surface, which made identification of small defects impossible. Other identified channel defect samples, however, showed an elliptic geometry in the cross sectional view. The size on the major axis of this ellipse was (10-15% larger than that on the minor axis. All inclusion defects were identified from the cross-sectional view. Shapes of these defects were also elliptic, and the size on the major axis, parallel to the sealing direction, was up to 3× larger than that on the minor axis.

BAI-mode images

The 17.3-MHz BAI-mode images of 14.5-μm air-filled (Fig. 6a) and 6.0-μm water-filled (Fig. 6b) channel defects were observed within the seal region of all-plastic retortable pouches. Of 12 channel defects within the all-plastic seals, two 6-μm air-filled and one 6-μm water-filled channel defects were not detected. The 9.6-μm air-filled (Fig. 6c) and 6.0-μm water-filled (Fig. 6d) channel defects were compared within the seal area of the foil-containing pouch. Of 12 channel defects, only one 6-μm water-filled channel was not detected. Thus, the 17.3-MHz BAI-mode imaging technique detect-

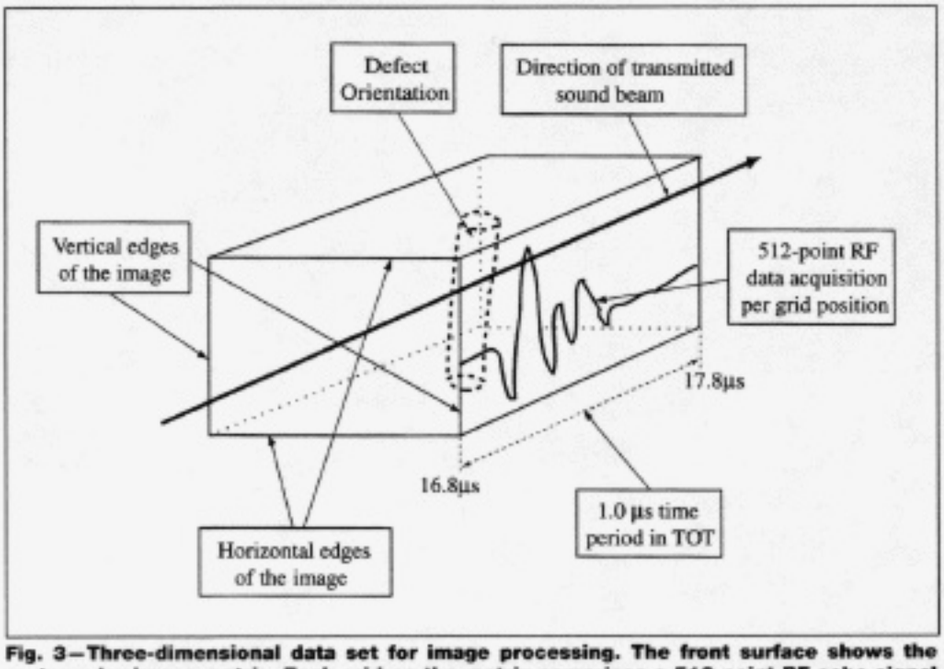

Fig. 3—Three-dimensional data set for image processing. The front surface shows the rectangular image matrix. Each grid on the matrix comprises a 512-point RF echo signal between TOT =16.8 and 17.8 µs. Direction of the sound beam is perpendicular to the image surface.

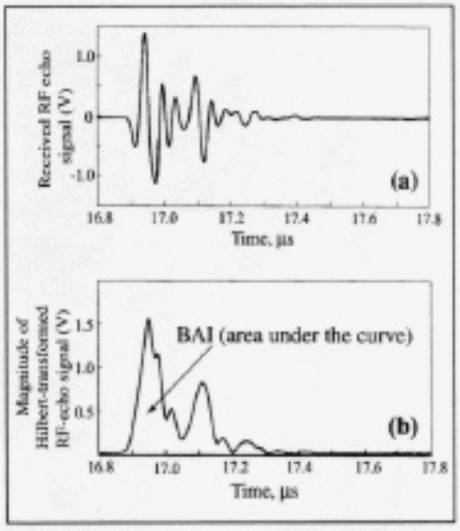

Fig. 4—(a) Raw RF echo signal obtained for each grid in the image matrix; (b) The magnitudes of Hilbert transformation of (a). The area under the curve in (b) results in BAI value.

ed all channel defects from 9.5 to 15.0 µm in diameter regardless of medium but it did not always detect the 6-µm defects.

In the 17.3-MHz BAI-mode image of tendons within the all-plastic seal areas (Fig. 7) smallest lateral sizes measured were about 20.0 µm (Fig. 7a) and 48.0 µm (Fig. 7b). In the BAI-mode image of the tendons within the foil-containing seal areas, since the foil-containing pouch was opaque, the optical size measurement after sealing was not possible from the top view. Instead, their size on the major axis of elliptical geometry was measured from the side view (Fig. 7, dashed lines). The sizes were about 22.6 (Fig. 7c) and 42.4 µm (Fig. 7d). From three samples fabricated for BAI-mode imaging, the minimum size (from ellipse major axis) of these inclusion defects within the foil-containing seals was 22.6 µm. Thus, the BAI-mode imaging technique detected tendon defects in both materials from 20 to 60 µm.

DISCUSSION

THE BAI VALUES OBTAINED AT THE NORmal incidence to the sound propagation direction were smaller in the channel leak and the tendon inclusion than in the undisturbed regions of both all-plastic and foil-containing pouches. Therefore, the defect region on the gray scale BAI-mode image appears as darker than the undisturbed region. Raum et al. (1998) and Ozguler et al. (1998) suggested the same findings for such normal-incidence conditions.

Since the elevated BAI values at the normal incidence of sound propagation were much closer to those in the undisturbed region than those in the defect region, the BAImax value on each image directly demonstrated the value from the undisturbed region. The BAImax value of 15 all-plastic and 15 foil-containing retort pouches with defects was determined from the corresponding BAI-value matrix. The calculated average and standard deviation of these BAImax values were 171.42±36.66 V-µs for all-plastic and 207.49±9.02 V-µs for foil-containing retortable pouches. Thus, the backscattered energy from the seal region of plastic pouches thickness of 220 µm was considerably less than that of foil pouches thickness of 240 µm (ANOVA analysis, $p<0.001$).

The coefficient of variation of the BAI_{max} values was 21.38% for the all-plastic retortable pouches and 4.35% for foil-containing retortable pouches. This reconfirms the visual observations of the seal region, i.e., in the foil-containing retortable pouches it was generally much smoother than in all-plastic retortable pouches. Variations of baseline BAI_{max} might be attributed to the heat seal processing conditions or packaging material. Therefore, this variation might be used as a quality and process control guideline if this imaging technique were implemented for on-line inspection of heat seal regions of flexible packaging materials.

Sizes of all channel defects on the 17.3-MHz BAI-mode image were (150-200 µm (Fig. 6) even though their actual size was less. This indicates the BAI imaging technique was limited for characterizing the defect in

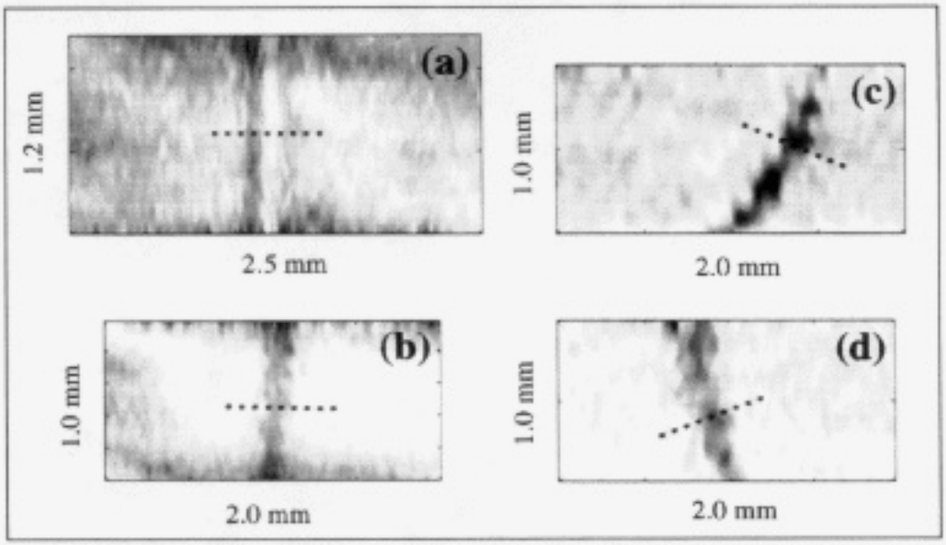

Fig. 5—Light transmission microscope image of 14.5-µm air-filled channel defect at 40× magnification (a); and tendon defect (20µm) at 10× magnification (b) within the seal area of the all-plastic pouch. Dashed lines show the location for the measurement.

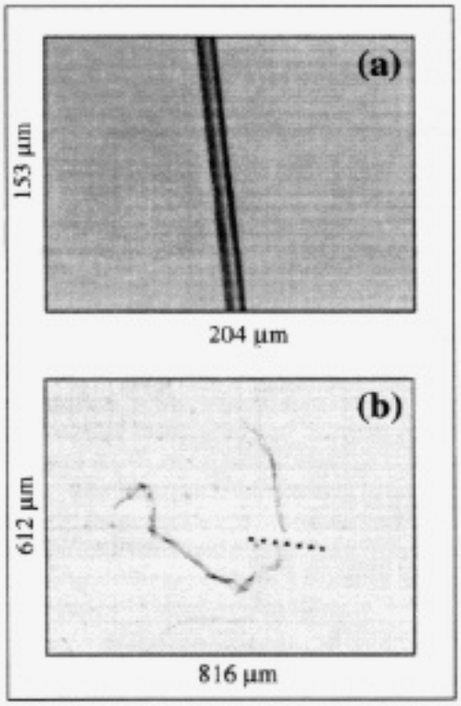

Fig. 6—BAI-mode image of (a) 14.5 µm air-filled channel defect within the all-plastic seal; (b) 6-µm water-filled channel defect within the all-plastic seal; (c) 9.6-µm air-filled channel defect within the foil-containing seal; (d) 6-µm water-filled channel within the foil-containing seal. Dashed lines show the location for the measurement.

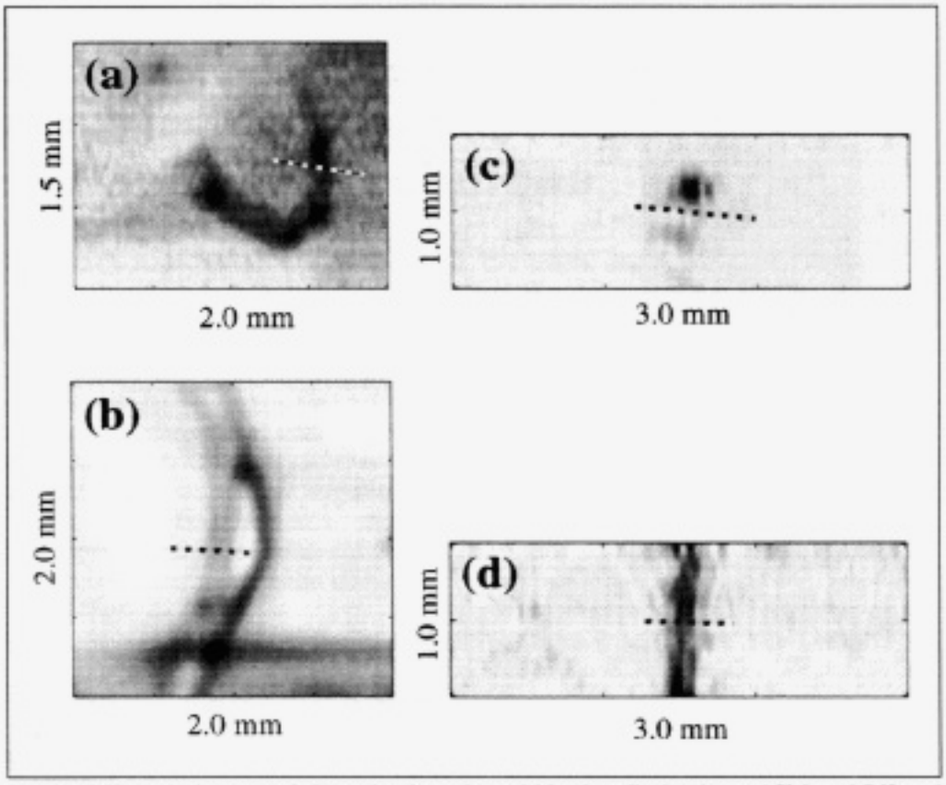

Fig. 7—BAI-mode images of the animal tendon within the all-plastic seal [(a) and (b)] and the foil-containing seal [(c) and (d)]. The light transmission microscope image of (a) is in Fig. 4(b). Dashed lines show the location for the measurement.

terms of size. This trend was consistent with all other channel defects. Raum and O'Brien (1997) measured the lateral resolution of tungsten wires (25- 80µm) by evaluating the -6 dB transmit-receive beam width in the true focal plane. They found that the lateral resolution of wires was about 176 µm for 17.3-MHz center frequency transducer. Sizes of the channel defects obtained by BAI-mode imaging (150-200 µm) were consistent with the reported lateral resolution. This is advantageous because the image of small defects would thus be magnified, and could easily be inspected even though the technique could not determine the size of the defect.

The transducer position during scanning was very important (Fig. 8). A defect channel "i" (50-µm air inclusion in the all-plastic seal region), the edge of seal region "ii", and separation zone of the material "iii" are shown (Fig. 8a). The variation of the BAI values in the direction transverse to the channel defect (I) (Fig. 8b) and in the direction transverse to the edge of the heat seal and separation region (II) (Fig. 8c) were compared. Even though the channel size (Fig. 8a) was very large (50 µm), identification was difficult because the BAI values in the defect region were between those in the seal edge and separation region [$BAI_{iii} > BAI_i > BAI_{ii}$]. As long as the BAI values on the defect approach the minimum BAI value in the image matrix, the defect would have high contrast on the image. If only the seal region (under line III) were scanned, i.e., the region above line III was removed from the image matrix, then the end result [$BAI_{iii} > BAI_i$] would bring about a high contrast and easily distinguishable channel defect on the new image matrix (Fig. 8d). These findings suggest that the transducer and sample should be positioned such that the scanning area includes only the seal region.

For the highly competitive food industry to implement new types of energy and cost-efficient flexible and rigid heat-sealed packages for shelf-stable food, a nondestructive 100% in-line package seal integrity inspection method is needed to ensure safety and to enable economic production, by accommodating the inspection bottleneck imposed by 9CFR§381.301(d). The method must be fast, robust and reliable, and not contaminate foods or pose a health hazard to plant personnel or customers. Nondestructive techniques such as X-ray and MRI do not sense air voids, which might cause microbial penetration into the packaged foods, even though these two techniques have high resolution (1.0 µm for X-ray and 30.0 µm for MRI) for electron dense materials (Harper et al., 1995). Pressure differential testing is a nondestructive technique to determine leakage, i.e., air voids, within the seal area (Floros and Gnanasekharan, 1992; Yam, 1995). However, other inclusions such as a food product within the seal area might result in the failure of a pressure differential test or gas "sniffer" device. Our results showed that unlike other nondestructive techniques, the high frequency (17.3 MHz) pulse-echo BAI-mode imaging technique is an effective way to visualize and evaluate both air-filled defects and occluded particles in the seal area.

In applying nondestructive evaluation in diagnostic ultrasound resolution must be considered along with depth of penetration. As the ultrasonic frequency is increased, resolution increases and penetration decreases. At the ultrasonic frequency (17.3 MHz) we used, the seal area of flexible food packages could be reliably inspected. However, if better resolution were desired, that could be achieved by increasing the ultrasonic frequency while keeping reasonable penetration depth (~0.2-0.4 mm) for detection of defects in the seal region. To improve resolution, research is needed to evaluate the BAI technique at higher ultrasonic frequencies.

CONCLUSION

HIGH-FREQUENCY ULTRASOUND IMAGING can provide the proper sensing method for the construction of a real-time, non-destructive package seal-integrity inspection device. Apparent limitations (such as the 6 µm lower limit of reliably produced defects) could readily be remedied by increasing the frequency. The apparent physical limitations of the method are related to the types of materials. High loss materials such as paper or low-density foams would disperse too much

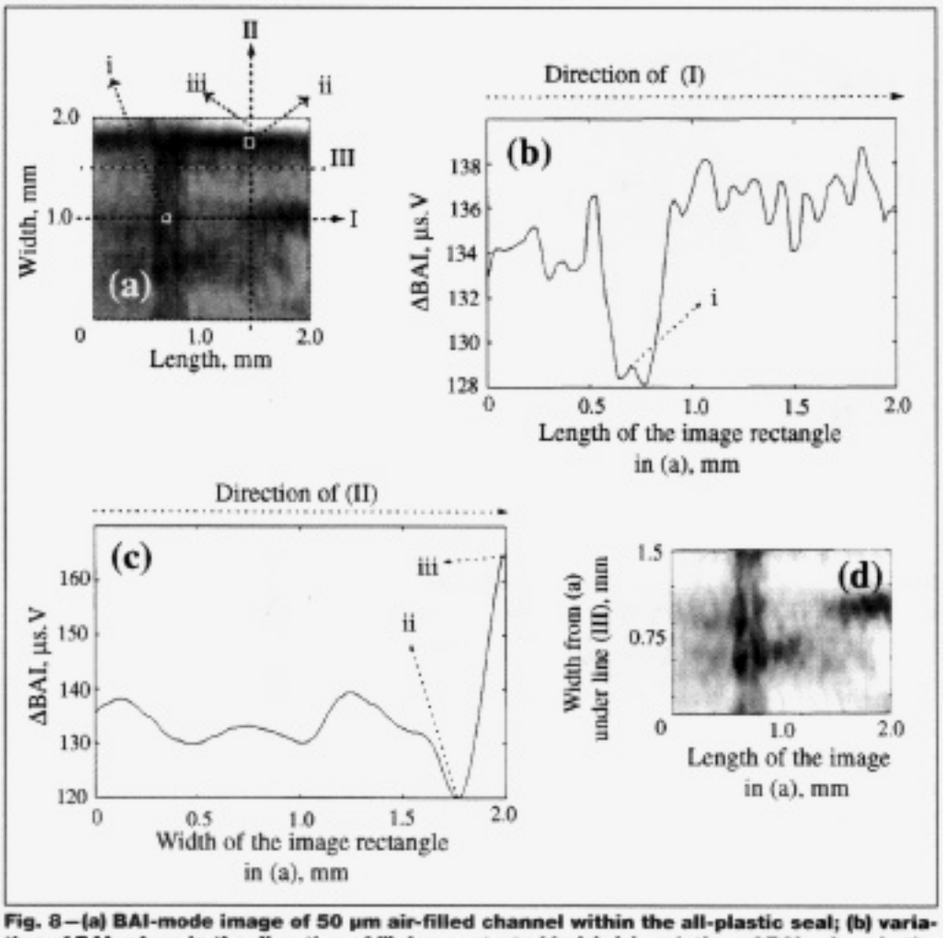

Fig. 8—(a) BAI-mode image of 50 μm air-filled channel within the all-plastic seal; (b) variation of BAI values in the direction of (I) demonstrated in (a); (c) variation of BAI values in the direction of (II); (d) BAI-mode image of the section under the line (III) illustrated in (a).

acoustic energy to provide a reliable imaging medium, but the low-density polyolefin films were inspected quite well. Materials of extreme thickness (several mm, outside the range of most food packaging) might cause loss problems. The method may be used to image any type of material, heatseal or artifact within such limitations. The method also exceeds the reliability of human inspectors by detecting defects that may be covered in opaque material or too small for visual detection.

REFERENCES

Axelson, L., Cavlin, S., and Nordst-rm, J. 1990. Aseptic integrity and microhole determination of packages by electrolytic conductance measurement. Pkg. Technol. & Sci. 3: 141-162.

Blakistone, A.B, Keller, S.W., Marcy, J.E., Lacy, G.H., Hackney, C.H., and Carter, W.H., Jr. 1996. Contamination of flexible pouches challenged by immersion biotesting. J. Food Protection 59(7): 764-767.

Chen, C., Harte, B., Lai, C., Pestka, J., and Henyon, D. 1991. Assessment of package integrity using a spray cabinet technique. J. Food Protection 54: 643-647.

Floros, J.D. and Gnanasekharan, V. 1992. Principles, technology and applications of destructive and nondestructive package integrity testing. In *Advances in Aseptic Processing Technologies*, R.K Singh and P.E. Nelson (Ed.), p.157-188. Elsevier Applied Science, New York, NY.

Frazier, C.H., Ozguler, A., Morris, S.A. and O'Brien, W.D., Jr. 1998. High-contrast images of defects in food package seals. Proc. 1997 IEEE Ultrasonics Symposium: In press.

Gnanasekharan, V. and Floros, J.D. 1994. Package integrity evaluation: Criteria for selecting a method. Pkg. Technol. & Engr. 3(6): 44-48.

Harper, C.L. 1995. A microbial challenge procedure for identification of defective flexible plastic pouch seals. Ch. 10 in *Plastic Package Integrity Testing Assuring Seal Quality*, B.A Blakistone and C.L. Harper (Ed.), p. 79-82. Institute of Packaging Professionals, Herndon, VA, USA.

Harper, C.L., Blakistone, B.S., Litchfield, J.B., and Morris, S.A. 1995. Developments in food package integrity testing. Food Technol. 6(10): 336-340.

Jarman, D., Farahbakhsh, and Herzig, R. 1994. Ultrasonic inspection of seal integrity of bond lines in sealed containers. U.S. patent 5,372,042.

Kinsler, L.E., Frey, A.R., Coppens, A.B., and Sanders, J.V. 1982. *Fundamentals of Acoustics*, John Wiley and Sons, New York.

Lampi, R.A., Schulz, G.L, Ciavarini, T., and Burke, P.T. 1976. Performance and integrity of retort pouch seals. Food Technol. 30: 38-48.

Ozguler, A., Morris, S.A. and O'Brien, W.D., Jr. 1998. Evaluation of defects in seal region of food packages using the Backscattered Amplitude Integral (BAI) technique. Proc. 1997 IEEE Ultrasonics Symposium: In press.

Paine, F.A. and Paine, H.Y. 1983. *A Handbook of Food Packaging*, Blackie & Son Ltd., Washington, DC.

Raum, K. and O'Brien, W.D., Jr. 1997. Pulse-echo field distribution measurement technique for high-frequency ultrasound sources. IEEE Transactions on Ultrasonics, Ferroelectrics and Frequency Control, 44(4): 810-815.

Raum, K., Ozguler, A., Morris, S.A., and O'Brien, W.D., Jr. 1998. Channel defect detection in food packages using integrated backscatter ultrasound imaging, IEEE Transactions on Ultrasonics, Ferroelectrics and Frequency Control: 45(1): 30-40.

Salvi, A.A., Meerbaum, H.J., Morris, S.A., Harper, C., and O'Brien, W.D., Jr. 1997. Acoustic imaging of defects in flexible food packages. J. Food Protection 60(3):309-314.

Szilard, J. 1987. Ultrasonics. In *Encyclopedia of Physical Science and Technology*, R.A. Meyers (Ed.), Vol. 14, p. 191-209. Academic Press, Inc., Orlando, FL.

Warrick, D. 1990. Aseptics: the problems revealed. Food Manufac. 65(10): 63-66.

Yam, K.L. 1995. Pressure differential techniques for package integrity inspection. Ch. 17 in *Plastic Package Integrity Testing Assuring Seal Quality*, B.A. Blakistone and C.L. Harper (Ed), p. 137-145. Institute of Packaging Professionals, Herndon, VA, USA.

Yamaguchi, K. 1990. Retortable packaging. In Food Packaging, Kadoya, T. (Ed.), p. 185-211. Academic Press, Inc., San Diego, CA.

Ms received 11/18/97; revised 2/20/98; accepted 2/25/98.

This work was supported in part by the Value-Added Research Opportunities Program, Agricultural Experiment Station, University of Illinois. We acknowledge the professional assistance with sample validation by James F. Zachary, DVM, Ph.D., Dept. of Veterinary Pathobiology, Univ. of Illinois. This work was presented in 1997 Annual Meeting of the Institute of Food Technologists, Orlando, FL.